

# Screening of point charge impurities in highly anisotropic metals: application to $\mu^+$ spin relaxation in underdoped cuprates

Arkady Shekhter, Lei Shu, Vivek Aji, D. E. MacLaughlin, C. M. Varma

*Department of Physics and Astronomy,  
University of California, Riverside, CA. 92521*

## Abstract

We calculate the screening charge density distribution due to a point charge, such as that of a positive muon ( $\mu^+$ ), placed between the layers of a highly anisotropic layered metal. In underdoped hole cuprates the screening charge converts the charge density in the metallic layers in the vicinity of the  $\mu^+$  to nearly its value in the insulating state. The current-loop ordered state observed by polarized neutron diffraction then vanishes near a  $\mu^+$  over the region of such cells as well as the nearby cells over a distance of order the intrinsic correlation length of the loop-ordered state. We calculate the magnetic field at the  $\mu^+$ -sites with such a suppressed order parameter, and find it reasonable that it is below the observation limit. This resolves the controversy between the neutron diffraction and muon spin relaxation ( $\mu$ SR) experiments. The screening calculation has relevance also for the effect of other charge impurities in the cuprates such as the dopants themselves.

In metals composed of metallic layers with negligible hopping from one layer to the next, the screening distance  $\lambda_s$  of a point charge placed between the layers depends on the distance  $c$  between the layers, the distance  $d$  of the charge to the layers and the electronic compressibility of the layers. Through an elementary calculation based on the Thomas-Fermi method, we obtain the screening charge distribution and discuss how it is modified in strongly correlated metals. The immediate occasion for doing such a calculation is that sensitive muon spin relaxation ( $\mu$ SR) experiments<sup>1,2,3</sup> have failed to detect the magnetic field in underdoped cuprates expected to be produced at the muon given the magnetic order observed by polarized neutron scattering.<sup>4,5,6</sup> The proposed loop current order parameter<sup>7,8</sup> is illustrated in Fig. 1.  $\mu$ SR experiments have been carried out in both underdoped  $\text{La}_{2-x}\text{Sr}_x\text{CuO}_4$ <sup>1</sup> and  $\text{YBa}_2\text{Cu}_3\text{O}_{6+x}$ .<sup>2,3</sup> The discrepancy is huge; the expected field at the muon site is about 50 G while recent experiments<sup>1</sup> put an upper limit of about 0.2 G.

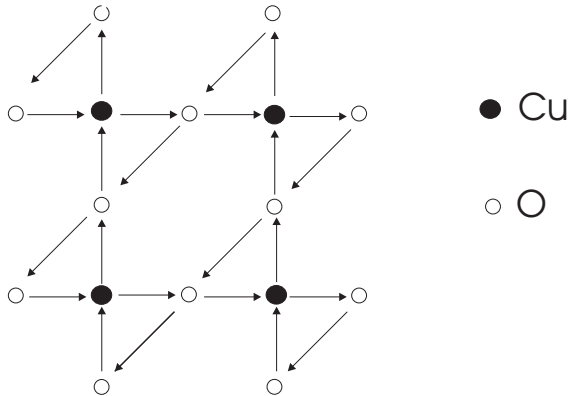


FIG. 1: The orbital current pattern in the  $\text{CuO}_2$  plane.

Loop-current magnetic order has been observed by polarized neutron diffraction experiments; the results on underdoped  $\text{YBa}_2\text{Cu}_3\text{O}_{6+x}$ <sup>4</sup> have been verified in an independent experiment.<sup>5</sup> Magnetic order of the same symmetry is also observed by neutron diffraction in underdoped  $\text{HgBa}_2\text{CuO}_4$ .<sup>6</sup> In both these compounds the observed order is long-range, limited only by the resolution of the experiment. In underdoped  $\text{La}_{2-x}\text{Sr}_x\text{CuO}_4$  only short-range order with a correlation length of about  $10 \text{ \AA}$  is observed (around the same Bragg spots and with similar integrated intensity as the other compounds),<sup>9</sup> due presumably to the larger charge disorder in this family of cuprates and the resultant effects discussed in this paper. [One may argue that it is therefore perhaps not the ideal cuprate compound to look for local fields. But even with a short correlation length  $\mu$ SR experiments, being local

probes, might have been expected to see effects which are not observed.] The magnitude of the ordered moment is large, estimated to be between 0.05 to 0.1  $\mu_B$  per O–Cu–O plaquette at about 10% doping, (decreasing to zero at the quantum critical point), or twice that for the sublattice magnetization per unit cell. Earlier dichroic ARPES results<sup>10</sup> on underdoped BISCCO samples revealed exactly the same symmetry of magnetic order. These experimental results were considered controversial,<sup>11,12,13</sup> but the neutron diffraction experiments lend them further credence. In underdoped  $\text{YBa}_2\text{Cu}_3\text{O}_{6+x}$ , a small dichroic signal characteristic of a time-reversal breaking order parameter has also been observed<sup>14</sup> and may be associated with a small ferromagnetic order accompanying the main loop-current order.<sup>15</sup>

On the basis of all these experiments, there are grounds now to believe that the loop-current order is universal in underdoped cuprates. It is therefore important to understand why  $\mu\text{SR}$  experiments see no sign of the magnetic order.

The loop-current order can occur only in a limited range of electron density, from about 5% to about 15% deviation of charge density from the half-filled band. Below about 5% doping the materials are antiferromagnetic insulators, while the quantum critical point at which the loop current order ends is at about 15% doping. The experiments are done with positively charged muons ( $\mu^+$ ), which unlike polarized neutrons are not innocent observers of a magnetic field. Their charge must be screened in the metal by displacing electrons from their vicinity with an integrated density equal to that of the  $\mu^+$  charge. We show that this makes cells in the metallic layers in the vicinity of the  $\mu^+$  acquire a local charge density characteristic of the insulator. This of course removes the order locally. But besides this effect, the magnitude of the loop-current order parameter is reduced around such cells over a distance of the order of the intrinsic correlation length of the ordered state (several lattice constants). We calculate the field expected at the  $\mu^+$  when these effects are included and find that it is below the observable limits.

We note that such screening does not occur in an insulator, where there is a gap to low energy charge excitations. Thus antiferromagnetism in the insulating state of the cuprates is perfectly well observed in  $\mu\text{SR}$  experiments.

Our elementary calculation and conclusion also has applications to other properties such as local one-particle spectra measured by STM as well as transport properties affected by charged defects in layered metals and superconductors.

We use the model of metallic layers specified by charge density of the typical underdoped

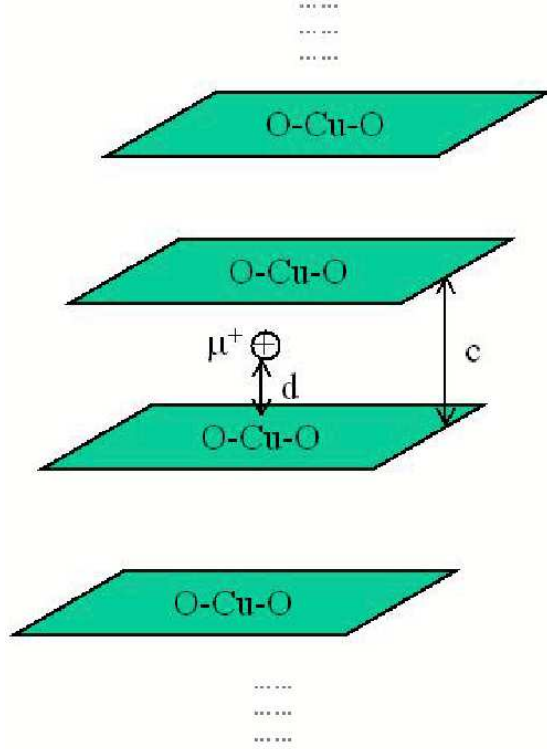


FIG. 2: Schematic of  $\text{CuO}_2$  layers and the  $\mu^+$  site.

cuprate, with a compressibility  $dn/d\mu$  and a separation from each other by a vertical distance of  $c$  (see Fig. 2). The positive charge is placed at a distance  $d < c$  above one of the layers. We use the Thomas-Fermi method to calculate the potentials and the charge density changes. The potential  $\phi(r, z)$  approximately follows the Poisson equation,

$$-\nabla^2\phi(\mathbf{r}, z) = 4\pi\frac{e}{\epsilon}(\rho_{\text{ext}}(\mathbf{r}, z) + \rho_{\text{ind}}(\mathbf{r}, z)). \quad (1)$$

$\epsilon$  has been introduced to account for static polarizability in between the layers. The long wavelength limit of  $\epsilon$  is known to be about 4.

The external charge is

$$\rho_{\text{ext}}(\mathbf{r}, z) = \delta(z - d)\delta(\mathbf{r}), \quad (2)$$

and the induced charge is given in the Thomas-Fermi approximation by

$$\rho_{\text{ind}}(\mathbf{r}, z) = -\frac{e^2}{\epsilon}(dn/d\mu)\phi(\mathbf{r}, z). \quad (3)$$

It is straightforward to show that the solution of these equations is such that the charge density  $\rho_n(r)$  on the  $n$ th layer can be obtained by numerically evaluating

$$\rho_n(r) = \int \frac{\xi d\xi}{2\pi} J_0(\xi r) \int_{-\pi/c}^{\pi/c} \frac{dk}{2\pi} e^{ikz_n} \rho(\xi, k),$$

where

$$\rho(\xi, k) = \frac{2\kappa_{2d} \bar{\rho}(k, \xi)}{1 + \frac{\kappa_{2D}}{\xi} \frac{\sinh \xi c}{\cosh \xi c - \cos kc}},$$

$$\bar{\rho}(k, \xi) = \frac{1}{2\xi} \frac{e^{-ikc} \sinh \xi d + \sinh \xi(c-d)}{\cosh \xi c - \cos kc},$$

and the response  $\kappa_{2d}$  is defined by

$$\kappa_{2d} \equiv 2\pi(e^2/\epsilon)(dn/d\mu). \quad (4)$$

In the general case, the screening charge distribution  $\rho_n(r)$  can only be obtained by numerical evaluation. Some features of interest may however be noted immediately. For a charged impurity near an isolated two dimensional conducting plane<sup>16</sup>, the screening charge density decays as  $\propto 1/r^3$ . For large enough  $\kappa_{2d}$ , (of the order or larger than the effective mass enhancement divided by  $\epsilon$  of about 1), the screening charge density is independent of  $\kappa_{2d}$  and only determined by the interplanar separation,  $c$ , and the distance of the charge to the plane,  $d$ . For the usual situation where  $d$  is close to  $c/2$ , the screening is determined entirely by the interplanar distance  $c$ . For  $\kappa_{2d} \rightarrow 0$ , the incompressible limit as in an insulator, there is no screening.

The calculated  $\rho_n(r)$  in the layers in the immediate vicinity of the  $\mu^+$  are shown in Fig. 3. The induced normalized charge density is a function of the radial distance, measured from directly below the  $\mu^+$ . More distant layers have negligible screening charge. A check on these calculations is that the integrated screening charge equals in magnitude the  $\mu^+$  charge. We have taken  $\kappa_{2d} \approx 10/c$ , estimated from an effective mass  $\approx 4 = \epsilon$ . The results are insensitive to the value of  $\kappa_{2d}$  beyond about  $10/c$ . For much smaller values of  $\kappa_{2d}$  than this, the screening distance goes up with a corresponding decrease of charge density immediately above and below the  $\mu^+$ . This is as it should be since for  $\kappa_{2d} \rightarrow 0$ , we should approach the insulating case.

There is an interesting general point about screening in strongly correlated material which is not directly covered by the Fermi-Thomas approximation. The screening charge in the

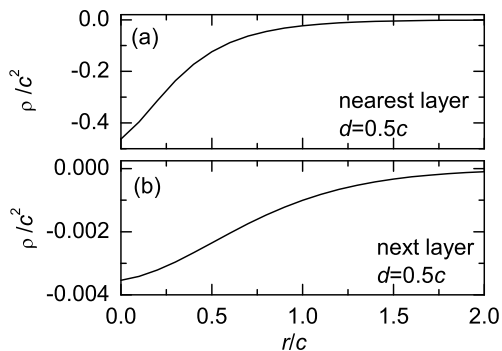


FIG. 3: The screening charge density in the layers in the immediate vicinity of the  $\mu^+$ . (a): Nearest neighbor plane. (b): Next nearest neighbor plane.

immediate vicinity of the charged defect in some parameter range, as discussed below, is such that the charge density crosses over past the charge density in the insulator to effective local electron-doping. The compressibility of the insulator is zero. So when the charge in a cell is well in the insulating regime, it cannot change into the 'electron' doping regime. Instead, the charge density will locally stay close to the 'zero-doping' and the screening charge will be distributed more evenly outside the cell in the immediate vicinity as well as increased in the more distant layer. Within the above scheme this may be simulated by a *local* response  $\kappa_{2d}[\rho(r)]$ , which goes to zero when  $\rho(r)$  is in the insulating regime. This has the effect of flattening the screening charge distributions compared to those shown in fig. 3.

We now apply the calculations to the parameters of underdoped LSCO. In this compound the layers are separated by  $c \approx 6.7 \text{ \AA}$  and the in-plane lattice constant is  $a \approx 3.8 \text{ \AA}$ . From Fig. 3, for the case  $d = 0.5c$  ( $\mu^+$  in the middle of the two planes), the integrated screening charge density in the cell immediately above and below the  $\mu^+$  changes by about 10% and in each of the adjoining 8 cells, it changes by about 5%, with negligible screening charge farther away. At a typical underdoping concentration of say 10%, this places the cells directly underneath definitely in the insulating regime and their neighbors close enough that the proposed orbital order is strongly affected in them from this effect alone. But as shown below there is another equally important effect to consider so that even the conversion of one of the cells to the insulating composition is enough to make the observation of the order by the muons unlikely.

For  $d = 0.3c$ , which is a large asymmetry in the placement of the  $\mu^+$ , the screening charge density in the nearest and the next nearest neighbor plane are shown in Fig. 4. The screening charge in cell in the nearest plane changes by about 30% and the 8 in the vicinity change by about 3%. The numbers in the plane in the other side are reduced correspondingly. As discussed above, the screening charge distribution in the closest plane must be more smoothly varying than in the Fermi-Thomas approximation.

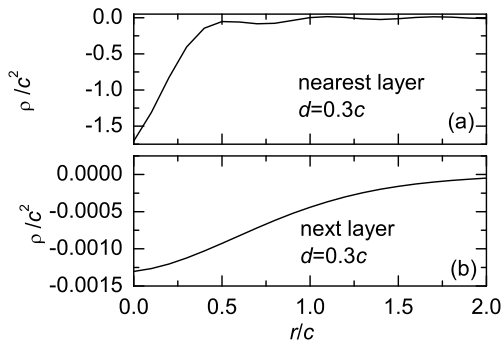


FIG. 4: The screening charge density in the layers which is a large asymmetry in the placement of the  $\mu^+$ . (a): Nearest neighbor plane. (b): Next nearest neighbor plane.

Consider now the effect on the spatial variation of the order parameter  $\Upsilon$  on reducing it to zero by the above effect in the metallic cells close to the  $\mu^+$ . The amplitude of the order parameter can only recover to its full value over the characteristic coherence length  $\xi$  of the order parameter  $\Upsilon(r)$  beyond the cells where  $\Upsilon$  vanishes. The spatial dependence of  $\Upsilon$  is determined by

$$\xi^2 \nabla^2 \Upsilon(\mathbf{r}) = \frac{\partial F_0}{\partial \Upsilon(\mathbf{r})}, \quad (5)$$

where  $F_0$  is the free energy of the homogeneous loop-order phase, with the boundary condition that  $\Upsilon$  is zero in the lattice cells close to the  $\mu^+$ . This equation also occurs in the context of the variation of the order parameter in the core of a vortex except that here the boundary condition  $\Upsilon(\mathbf{r}=0) = 0$  is replaced by  $\Upsilon(\mathbf{r}) = 0$  for  $\mathbf{r} \lesssim a_0$ , the radius in which the local charge density is in the insulating range. At low temperatures  $\xi \approx a(E_e/E_{cl})^{1/2}$ , where  $a$  is the in-plane lattice constant,  $E_e$  is a typical electronic energy, say the conduction electron bandwidth  $O$  1 eV, and  $E_{cl}$  is the condensation energy of the loop-order phase.

Even if we take for the latter a value as high as 0.1 eV,  $\xi$  is about  $3a$ . Near the ordering temperature  $\xi(T)$  diverges.

This means that the magnitude of the order parameter at low temperatures is negligible in a range of order at least 2 lattice constants beyond the cells where it is truly zero. Since one to two cells immediately below the  $\mu^+$  have zero order parameter, it is reasonable to consider the magnetic field at the  $\mu^+$  site to be coming from cells of the layers in the immediate vicinity excluding 3 to 4 radially outwards from the one immediately below or above the  $\mu^+$ , for the case of nearly symmetric placement of the  $\mu^+$ . Actually, if only the cell immediately below and above the  $\mu^+$  in the two layers and one set of cells around this (9 cells in each layer) have negligible order parameter, the field at the  $\mu^+$  is below the observable limits as shown below.

The specific calculation is done by setting up an orthorhombic lattice, placing a  $\mu^+$  site and local moments in a magnetic structure in the unit cell, and summing over the local moments out to a given radius. The  $\mu^+$  is placed 1 Å below the apical oxygen, as suggested by muon experts<sup>17</sup>. With no change in the order parameter due to screening of the  $\mu^+$ , the field at the  $\mu^+$  for a magnetic order with a moment of  $0.05\mu_B$  per triangular plaquette placed at the centroid of the triangles is about 120 G in LSCO; (Macdougall et al.<sup>1</sup> obtain 41 G, due to a more precise calculation of the field due to the current pattern.) If we now exclude 9 cells in the immediate vicinity of the  $\mu^+$  site in each of the two layers, i.e.  $(a_0 + \xi) = 2$  lattice parameters (7.6 Å), the calculated magnetic field of about 1 G. When the next neighboring set of cells are excluded, i.e.  $(a_0 + \xi) = 3$  lattice parameters (11.4 Å) the field is about 0.5 G, while for  $(a_0 + \xi) = 4$  lattice parameters (15.2 Å) it is about 0.3 G. The unscreened field is about 50 Gauss if the  $\mu^+$  is placed at 1.2 Å below the apical oxygen with O(2) changes from those calculated above also for the screened case. The principal point is that the field at the muon is reduced by more than two orders of magnitude due to the inescapable effects (screening and finite stiffness for the variation of the order parameter) considered here. The precise values vary with the details like the muon position which are not accurately known.

The above does not take into account the small correlation length found for the loop order in LSCO, which would reduce all numbers by another order of magnitude. We have also calculated the effect of screening on the magnetic field at the muon for the structure of  $YBa_2Cu_3O_{6+\delta}$ . We find that the "unscreened field" for the muon at 1 Å below the apical oxygen and the same magnetic moment as above is about 600 G but the reduction due to

screening puts it at 3 G when only the cells immediately above and below the muon are excluded, and about 0.7 G when two neighboring cells in their vicinity are also excluded.

The lattice cells near  $\mu^+$  sites with charge density close to that of the insulator will acquire local spin moments at Cu sites, but given the small size of such regions thermal and quantum fluctuations do not allow any order. A number of zero-field  $\mu$ SR experiments in under- and optimally-doped  $\text{YBa}_2\text{Cu}_3\text{O}_{6+x}$  (Refs. 18,19) and  $\text{La}_{2-x}\text{Sr}_x\text{CuO}_4$  (Refs. 18,19,20) give evidence for weak dynamic relaxation at temperatures well above the superconducting transition. From the field dependence of this dynamic relaxation in  $\text{La}_{1.885}\text{Sr}_{0.115}\text{CuO}_4$  Watanabe et al.<sup>20</sup> infer a  $\sim 2$  G field fluctuating at a very slow rate (0.1 MHz). Although a strongly antiferromagnetically-coupled  $\mu^+$ -induced Cu spin “cluster” might be expected to fluctuate slowly, at present the dynamics of such a cluster are not sufficiently well understood to allow comparison with experiment. Such a coupled-spin cluster should, however, have a paramagnetic response appropriate to its net moment, which should lead to a  $\mu^+$  Knight shift proportional to  $1/T$  when an external magnetic field is applied. This temperature dependence is quite different from that expected from bulk susceptibility measurements.

Such  $\mu^+$  Knight shift experiments have not yet been carried out.<sup>21</sup> Transverse-field  $\mu$ SR experiments have, however, detected inhomogeneous static distributions of  $\mu^+$  fields with widths proportional to the applied field.<sup>3</sup> E.g., muons see a field-induced distribution of inhomogeneous magnetic fields with a spread of about 2 G at a field of 3 T. Suppose there is a  $1 \mu_B$  moment produced in the insulating cell above and below the  $\mu^+$ . With a Curie susceptibility, it produces an extra magnetic field at the  $\mu^+$  site of  $O(\mu_B H/T)\mu_B/|r|^3$ , where  $|r|$  is a typical distance to the  $\mu^+$  of about 5 Å and  $H$  is the applied field. At a field of 3 T and a temperature 100K, this field is about 100 G. If we allow a distribution of the detailed position of the muons due to local strains, a field distribution with a width  $\propto (1/T)H$  is expected in the normal state. Such a behavior is consistent with the observations<sup>3</sup>. The characteristic width of about 2G at 100 K is also consistent with our ideas. To test them further, a  $\mu^+$  Knight shift  $\propto 1/T$  should be looked for.

---

<sup>1</sup> G.J. MacDougall, A.A. Aczel, J.P. Carlo, T. Ito, J. Rodriguez, P.L. Russo, Y.J. Uemura, S. Wakimoto, and G.M. Luke. *Cond-mat*, 0801.2716, 2008.

- <sup>2</sup> J.E. Sonier, F.D. Callaghan, Y. Ando, R.F. Kiefl, J.H. Brewer, C.V. Kaiser, V. Pacradouni, S.A. Sabok-Sayr, X.F. Sun, S. Komiya, W.N. Hardy, D.A. Bonn, and R. Liang. *Phys. Rev. B*, 76:064522, 2007.
- <sup>3</sup> J.E. Sonier, M. Ilton, V. Pacradouni, C.V. Kaiser, S.A. Sabok-Sayr, Y. Ando, S. Komiya, W.N. Hardy, D.A. Bonn, R. Lian, and W.A. Atkinson. *Cond-mat*, 0801.3481, 2008.
- <sup>4</sup> B. Fauque, Y. Sidis, V. Hinkov, S. Pailhès, C. T. Lin, X. Chaud, and P. Bourges. *Phys. Rev. Lett.*, 96:197001, 2006.
- <sup>5</sup> H. Mook. In *Bulletin of American Physical Society March Meeting*, 2008.
- <sup>6</sup> Yuan Li, Victor Baledent, Neven Barisic, Philippe Bourges, Yongchan Cho, Benoit Fauque, Yvan Sidis, Guichuan Yu, Xudong Zhao, and Martin Greven, 2008.
- <sup>7</sup> C.M. Varma. *Phys. Rev. Lett.*, 83:3538, 1999.
- <sup>8</sup> C.M. Varma. *Phys. Rev. B*, 73:155113, 2006.
- <sup>9</sup> P. Bourges. Private Communication.
- <sup>10</sup> A. Kaminski, S. Rosenkranz, H. M. Fretwell, J. C. Campuzano, Z. Li, H. Raffy, W. G. Cullen, H. You, C. G. Olson, C. M. Varma, and H. Hochst. *Nature*, 416:610, 2002.
- <sup>11</sup> S.V. Borisenko, A.A. Kordyuk, A. Koitzsch, M. Knupfer, J. Fink, H. Berger, and C.T. Lin. *Nature*, 431:1, 2004.
- <sup>12</sup> J.C. Campuzano, A. Kaminski, S. Rosenkranz, and H.M. Fretwell. *Nature*, 431:2, 2004.
- <sup>13</sup> C.M. Varma. *Phys. Rev. B*, 73:233102, 2006.
- <sup>14</sup> Jing Xia, Elizabeth Schemm, G. Deutscher, S.A. Kivelson, D. A. Bonn, W. N. Hardy, R. Liang, W. Siemons, G. Koster, M. M. Fejer, and A. Kapitulnik. *Cond-mat*, 0711.2494, 2008.
- <sup>15</sup> V. Aji, A. Shekhter, and C.M. Varma. unpublished.
- <sup>16</sup> F. Stern. *Phys. Rev. Lett.*, 18:546, 1967.
- <sup>17</sup> J.H. Brewer, R.F. Kiefl, J.F. Carolan, P. Dosanjh, W.N. Hardy, S.R. Kreitzman, Q. Li, T.M. Riseman, P. Schleger, H. Zhou, E.J. Ansaldo, D.R. Noakes, L.P. Lee, G.M. Luke, Y.J. Uemura, K. Hepburn-Wiley, and C.E. Stronach. *Hyperfine Interactions*, 63:177, 1990.
- <sup>18</sup> J.E. Sonier, J.H. Brewer, R.F. Kiefl, R.I. Miller, G.D. Morris, C.E. Stronach, J.S. Gardner, S.R. Dunsiger, D.A. Bonn, W.N. Hardy, R. Liang, and R.H. Heffner. *Science*, 292:1692, 2001.
- <sup>19</sup> J.E. Sonier, J.H. Brewer, R.F. Kiefl, R.H. Heffner, K.F. Poon, S.L. Stubbs, G.D. Morris, R.I. Miller, W.N. Hardy, R. Liang, D.A. Bonn, J.S. Gardner, C.E. Stronach, and N.J. Curro. *Phys. Rev. B*, 66:134501, 2002.

<sup>20</sup> I. Watanabe, T. Adachi, S. Yairi, Y. Koike, and K. Nagamine. unpublished.

<sup>21</sup> J.E. Sonier. Private Communication.